ATL-PHYS-PROC-2011-131
28 September 2011

September 28, 2011

Diffractive and Low-X Physics at ATLAS

Tim Martin[1]

School of Physics and Astronomy, University of Birmingham,
B15 2TT, United Kingdom.

A brief overview of soft diffractive physics from colour singlet exchange at ATLAS is presented. The use of an exclusive single-sided trigger and of searches for large rapidity gaps in the final state are shown to be effective methods for studying the diffractive component of the total inelastic cross section in high energy *pp* collisions. Large rapidity gaps are spoiled by soft gluon emission from multi parton interactions, it is shown that the probability MPI in soft diffractive interactions is very small due to the characteristic large impact parameter in such events.

On the scale of pertubative QCD, the study of a jet veto in the rapidity interval bounded by a dijet system is presented. Colour singlet exchange is expected to become increasingly important in the joint limit that the rapidity separation of the bounding jets is large and that the mean transverse momentum of the dijet system is large, compared to the jet veto scale in the rapidity interval between them. In this regime the disagreement between data and theory is most pronounced.

PRESENTED AT

MPI LHC 2010
Glasgow, United Kingdom, November 29–December 03, 2010

[1]On behalf of the ATLAS collaboration.

1 Introduction

Typical charged particle yields in inelastic pp collisions at $\sqrt{s} = 7$ TeV are around 6 charged particles with transverse momentum* $p_{\mathrm{T}} > 100$ MeV per unit of pseudorapidity in the region $|\eta| < 2.5$ [1]. It therefore follows that the average particle-particle separation is expected to be around $\Delta\eta = 0.16$ with larger separations between neighbouring particles occurring as the result of fluctuations in the hadronisation process. The PYTHIA Monte Carlo (MC) simulation utilises the Lund string model of hadronisation [2] in which the production of large rapidity gap fluctuations are suppressed by an exponential factor.

An alternate process which can result in large rapidity gaps in the final state is the exchange of a propagator corresponding to the rightmost vacuum singularity in the complex angular momentum plane, more commonly referred to as the *Pomeron* ($I\!\!P$). The $I\!\!P$ is strongly interacting yet colour neutral, the lack of colour flow between the two protons gives rise to the possibility for the formation of large rapidity gaps (LRGs) and events involving the exchange of a $I\!\!P$ are often termed *diffractive*.

2 Kinematic Variables

In $pp \to XY$ events, classed as *double diffractive* (DD), both protons dissociate into masses M_X and M_Y with $M_Y < M_X$ by choice. In $pp \to pX$ or $pp \to Xp$ *single diffractive* (SD) events, one of the protons dissociates into the diffractive mass M_X. The recoil proton remains intact so that $M_Y = M_p$.

We define $\xi_X = M_X/s$ where s is the square of the centre of mass energy of the collision, ξ_X corresponds to the fractional momentum loss of the leading proton. At $\sqrt{s} = 7$ TeV, ξ_X spans over seven orders of magnitude - starting from the low mass limit of $\log_{10}(\xi_X) = -7.6$ for $M_X = M_p + M_\pi$. Large diffractive masses are limited by the coherence condition, $\xi_X \leq (M_p R)^{-1}$, here R represents the interaction length. Taking $R = M_\pi^{-1}$, this gives an upper limit of $\log_{10}(\xi_X) \lesssim -0.8$ [3].

In the triple Regge model [4], the approximate behaviour of the cross section is $d\sigma/dM_X^2 \propto 1/M_X^2$. This dependence is implemented in the PYTHIA 6, PYTHIA 8 and PHOJET MC generators and leads to the approximately constant cross section as a function of $\log_{10}(\xi_X)$ as plotted in Figure 1(a). In PYTHIA 6, proton dissociation occurs through hadronisation of a longitudinally stretched string between either the (valence) quark–di-quark or quark–gluon–di-quark system. PYTHIA 8 improves upon this model by including a modelling of hard diffraction for events with $M_X \gtrsim 10$ GeV. This is based on a partonic treatment of the $I\!\!P$ with Pomeron structure functions as measured in ep collisions by the H1 experiment at the HERA collider [5]. This leads

*Transverse momentum is with respect to the beam which runs along the z axis.

to a harder $p_{\rm T}$ spectrum within the diffractive system [6]. PHOJET also includes a hard diffractive component though a dual-parton model [7].

In SD events, the size of the gap between the scattered proton and dissociated system is defined $\Delta\eta = -\ln(\xi_X)$. We define the edge of the diffractive system to be the pseudorapidity of the particle closest to the scattered proton and label this $\eta_{\rm MIN}$. Figure 1(b) plots $\eta_{\rm MIN}$ as a function of $\log_{10}(\xi_X)$ for the PYTHIA 8 MC, the above relation is observed to hold on average though with some smearing due to hadronisation effects.

The probability of Multi Parton Interactions (MPI) occurring in the soft interactions described in this note are small, this is due to diffractive collisions being highly peripheral in nature. The pp impact parameter $b \sim 1/t$ (t is the squared four-momentum transfer) and the cross section for diffractive processes is vastly dominated by modest values of $|t| \lesssim 1$ GeV^2 such that in the SD case, the intact proton is only scattered through a very small angle. The same cannot be said for hard diffractive scatters at the LHC with a smaller impact parameter, here the probability of soft gluon radiation in the gap from MPI is expected to be large [8].

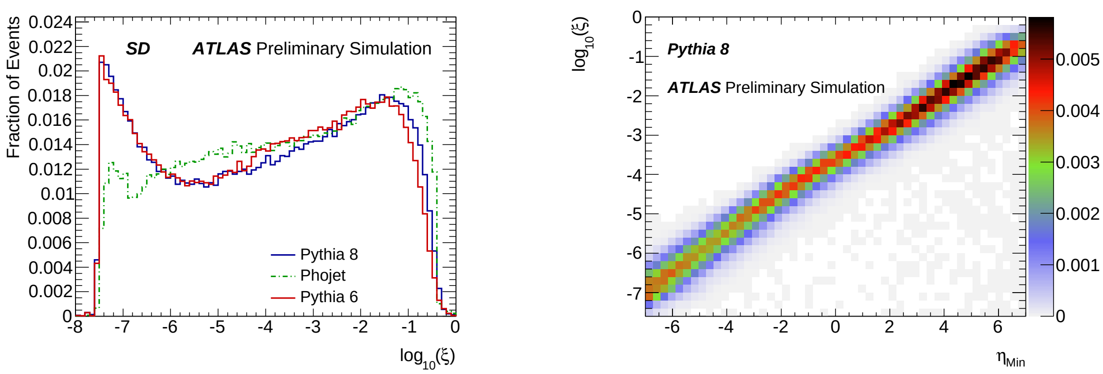

(a) SD Cross Section

(b) $\eta_{\rm MIN}$ Distribution

Figure 1: (a) Cross section for SD events for different MC generators as a function of $\log_{10}(\xi_X)$, normalised to 1. (b) Pseudorapidty of the particle which forms the edge of the diffractive system in SD events for the PYTHIA 8 generator where the dissociated proton is always travelling in the negative z direction. Both from ATLAS note [9].

3 The ATLAS Detector

The ATLAS detector is described in detail elsewhere [10]. Systems important to this discussion are the minimum bias trigger scintillators (MBTS), inner detector (ID), liquid argon sampling calorimeter (LAr) and hadronic tile calorimeter systems. The MBTS consists of 16 sensitive scintillator counters located either side of the interaction point covering $2.09 < |\eta| < 3.84^{\dagger}$, the MBTS is the primary physics trigger during low luminosity data taking. The ID covers $|\eta| < 2.5$, it consists of three tracking detectors, the silicon pixel detector, the silicon micro strip tracker and the transition radiation tracker. The LAr calorimeter systems hermetically cover the region $|\eta| < 4.9$, the scintillator/steel hadronic tile calorimeter covers the region $|\eta| < 1.7$.

The efficiency of the MBTS at triggering diffractive events is studied in MC. As shown in Figure 2, the MBTS is expected to be 50% efficient at triggering events by $\log_{10}(\xi_X) = -5.5$ which corresponds to $M_X \cong 12.4$ GeV.

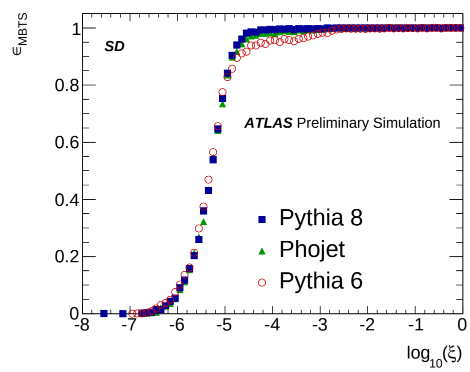

Figure 2: Efficiency of MBTS trigger in MC as a function of $\log_{10}(\xi_X)$. From ATLAS note [9].

4 Diffractive Enhanced Measurements

The following is a summary of the preliminary result [11]. An enhanced diffraction event sample was selected by requiring at least one MBTS counter above threshold on one side of the detector and exactly zero counters above threshold on the opposite side of the detector in z. This requirement preferentially selects intermediate mass SD events as well as DD events in which a intermediate mass M_X system occupies one side of the MBTS trigger while the mass of the Y system, M_Y, is sufficiently small that all particles escape at $|\eta| > 3.84$. Further, events are required to contain at least one charged particle with $p_T > 500$ MeV and $|\eta| < 2.5$. For such a selection the MBTS trigger efficiency is above 97% for all inelastic processes. The tracking efficiency of charged prompt hadrons is around 87% at central η, falling with increasing $|\eta|$ to around 65% at $|\eta| = 2.5$ [1]. The following distributions are plotted at the detector level:

†The acceptance of the MBTS, ID and calorimeter systems is taken with respect to the nominal $z = 0$ of the ATLAS detector. Track η is defined based on track perigee position.

$$\frac{1}{N_{ev}}\frac{dN_{trk}}{d\eta}, \frac{1}{N_{ev}}\frac{dN_{ev}}{dN_{trk}}, \frac{1}{N_{ev}}\frac{1}{2\pi p_{\mathrm{T}}}\frac{d^2N_{trk}}{d\eta dp_{\mathrm{T}}}, \frac{1}{N_{ev}}\frac{dN_{trk}}{d\Delta\eta}.$$

Here N_{ev} is the number of events satisfying the single-sided trigger plus the one or more charged particles requirement, p_{T} is transverse momentum of a reconstructed charged particle, η is the pseudorapidity of a reconstructed charged particle, N_{trk} is the number of reconstructed charged particles in an event ($p_{\mathrm{T}} > 500$ MeV) and $\Delta\eta$ is defined as the pseudorapidity gap between the edge of the MBTS detector which had no counters above threshold and the charged particle so $\Delta\eta = |\eta_{\mathrm{MBTS}} - \eta|$ where $\eta_{\mathrm{MBTS}} = \pm 2.08$ depending on which side of the detector did not have any counters above threshold. This distribution is plotted where $\eta > \eta_{\mathrm{MBTS}}$ ($\eta < \eta_{\mathrm{MBTS}}$) for $\eta_{\mathrm{MBTS}} < 0$ ($\eta_{\mathrm{MBTS}} > 0$). We expect $\Delta\eta$ to be peaked to large values for SD and DD events with a LRG which satisfies the single-sided trigger requirement. Plots are presented in Figures 3, 4 and 5, systematics from tracking uncertainty and MBTS response are included. We observe that PYTHIA 6 underestimates the particle multiplicity and p_{T} spectrum as expected due to its lack of a hard diffractive component. PYTHIA 8 is observed to agree better with data and PHOJET to provide the best agreement over the majority of the distributions.

5 Gaps Between Jets

The ATLAS publication [12] investigates the fraction of dijet events which survive the veto of a third jet with $p_{\mathrm{T}} > Q_0$ between the boundary jets (where $Q_0 = 20$ GeV). The fraction surviving this veto is presented for boundary jets separated by a rapidity interval (Δy) up to 6 and with mean transverse momentum $50 < \overline{p}_T < 270$ GeV. The dijet system is taken to be the two leading p_{T}-jets in the event and the fraction of events surviving the veto is referred to as the gap fraction. As the veto scale, Q_0, is chosen to be much greater than Λ_{QCD}, this allows phenomena in pertubatative QCD to be studied in regions of phase space which may not be adequately described by MC. BFKL-like [13] dynamics are expected to become increasingly important for large rapidity intervals while wide-angle soft-gluon radiation effects are studied in the limit that $\overline{p}_T$ of the dijet system is much larger than the veto scale. Colour singlet exchange is expected to be important when both criteria are simultaneously met.

Jets were reconstructed using the anti-k_t algorithm with distance parameter $R = 0.6$ and requirements $p_{\mathrm{T}} > 20$ GeV and rapidity $|y| < 4.4$. Data are corrected to a hadron level definition where jets are reconstructed from all final state particles (proper lifetime > 10 ps).

For large $\overline{p}_T/Q_0$ or Δy it is predicted that fixed order calculations are unlikely to be able to describe the data, rather resummation to all orders in perturbation theory

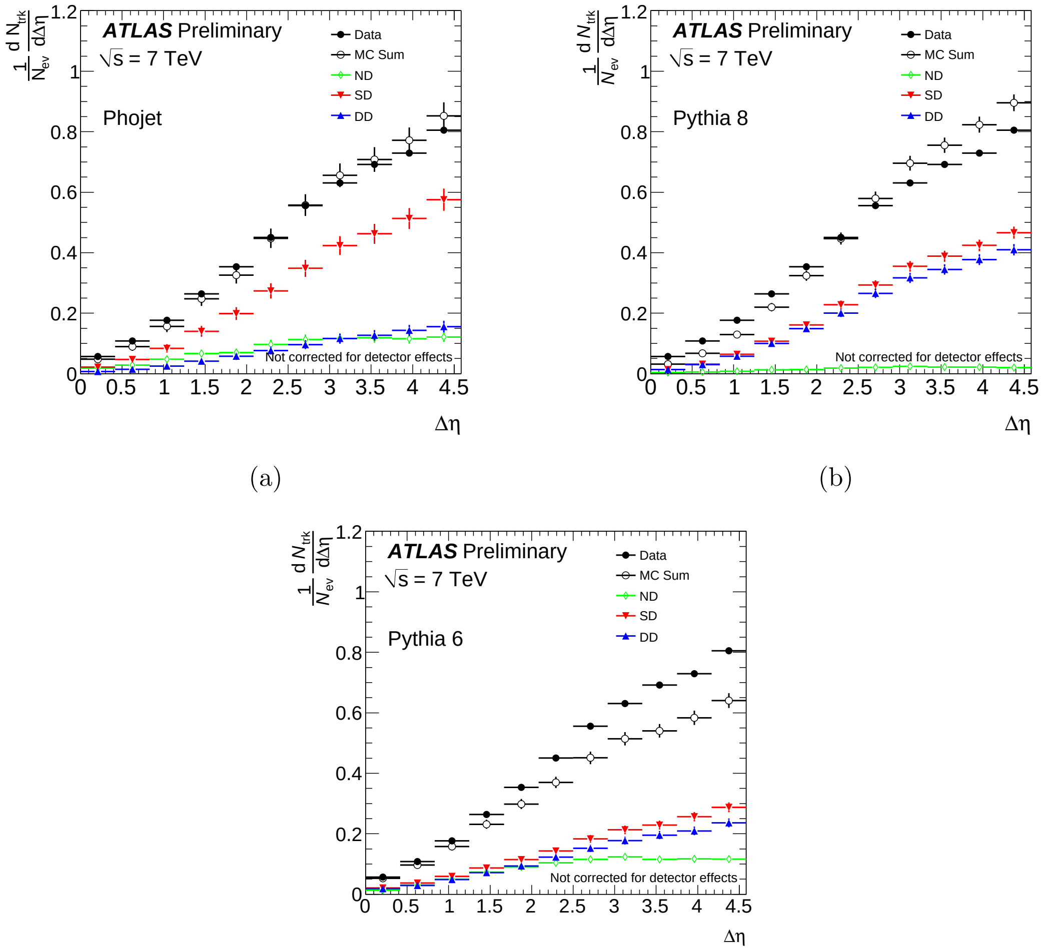

(a) (b)

(c)

Figure 3: $\frac{1}{N_{ev}}\frac{dN_{trk}}{d\Delta\eta}$ for the single-sided trigger requirement. MC normalised to default generator predictions. The sum of the three MC predictions is in open circles, data are in filled circles.

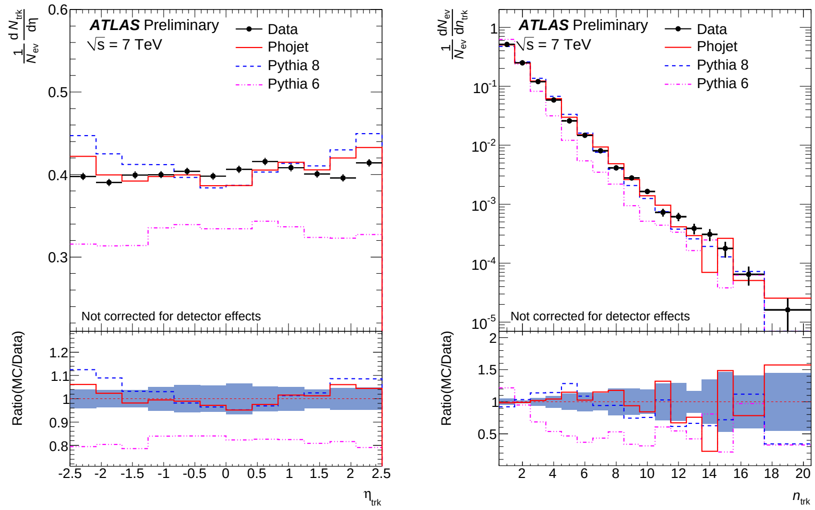

(a) (b)

Figure 4: $\frac{1}{N_{ev}}\frac{dN_{trk}}{d\eta}$ and $\frac{1}{N_{ev}}\frac{dN_{ev}}{dN_{trk}}$ for the single-sided trigger requirement. Data in black compared to MC models with default mixing of inelastic events.

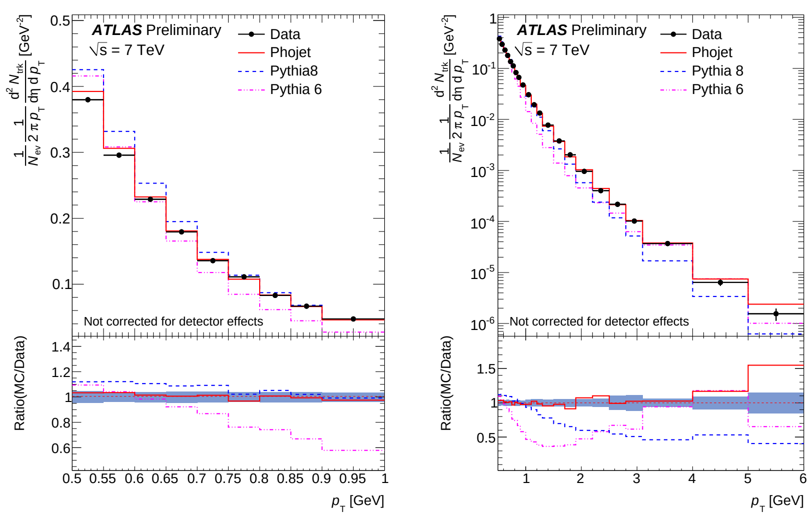

(a) (b)

Figure 5: $\frac{1}{N_{ev}}\frac{1}{2\pi p_{\mathrm{T}}}\frac{d^2N_{trk}}{d\eta dp_{\mathrm{T}}}$ for the single-sided trigger requirement and with two p_{T} ranges. Data in black compared to MC models with default mixing of inelastic events.

is required. The HEJ [14] and POWHEG-BOX [15] generators are compared with data. The HEJ generator provides an all-order description of wide-angle emission which is of similar p_{T}. In a BFKL-inspired limit, HEJ is expected to be especially suited to events with a large rapidity separation. POWHEG-BOX provides a full next-to-leading order dijet calculation, it is interfaced with PYTHIA (tune AMBT1) or HERWIG (tune AUET1) for all-order resummation of soft and collinear emissions under the parton shower approximation. With both generators, the MSTW 2008 NLO PDF set was used and the renormalisation scale in was set to the p_{T} of the leading parton.

Data are compared to HEJ, POWHEG+PYTHIA and POWHEG+HERWIG in Figure 6. HEJ gives a good description of Δy in the regime $\overline{p}_T \sim Q_0$ as per its design; discrepancies are observed when the dijet scale is much larger than Q_0. POWHEG+PYTHIA provides the best description but is also observed to deviate at large Δy where the NLO-plus-parton shower approximation becomes less valid. The spread of LO predictions from the PYTHIA, ALPGEN and HERWIG++ generators is also large, this demonstrates the large uncertainty in the theoretical predictions [16].

6 Conclusion

The selection of events containing LRGs is shown to be an effective method of exponentially suppressing non-diffractive inelastic interactions allowing for the kinematics of diffraction to be studied in detail. Precision measurements in ATLAS of diffractive dominated quantities will allow for a better phenomenological description of these non-perturbative QCD processes. At high p_{T}, dijet systems with large rapidity separation allow the study of another regime in which colour singlet exchange is expected to be important.

References

[1] ATLAS Collaboration, G. Aad et al., *Charged-particle multiplicities in pp interactions measured with the ATLAS detector at the LHC*, New J.Phys. **13** (2011) 053033, `arXiv:1012.5104 [hep-ex]`.

[2] T. Sjostrand, S. Mrenna, and P. Z. Skands, *PYTHIA 6.4 Physics and Manual*, JHEP **05** (2006) 026, `arXiv:hep-ph/0603175`.

[3] UA5 Collaboration, R. E. Ansorge et al., *Diffraction dissociation at the CERN pulsed collider at cm energies of 900 and 200 GeV. oai:cds.cern.ch:172602*, Z. Phys. C **33** (Jul, 1986) 175–185. 21 p.

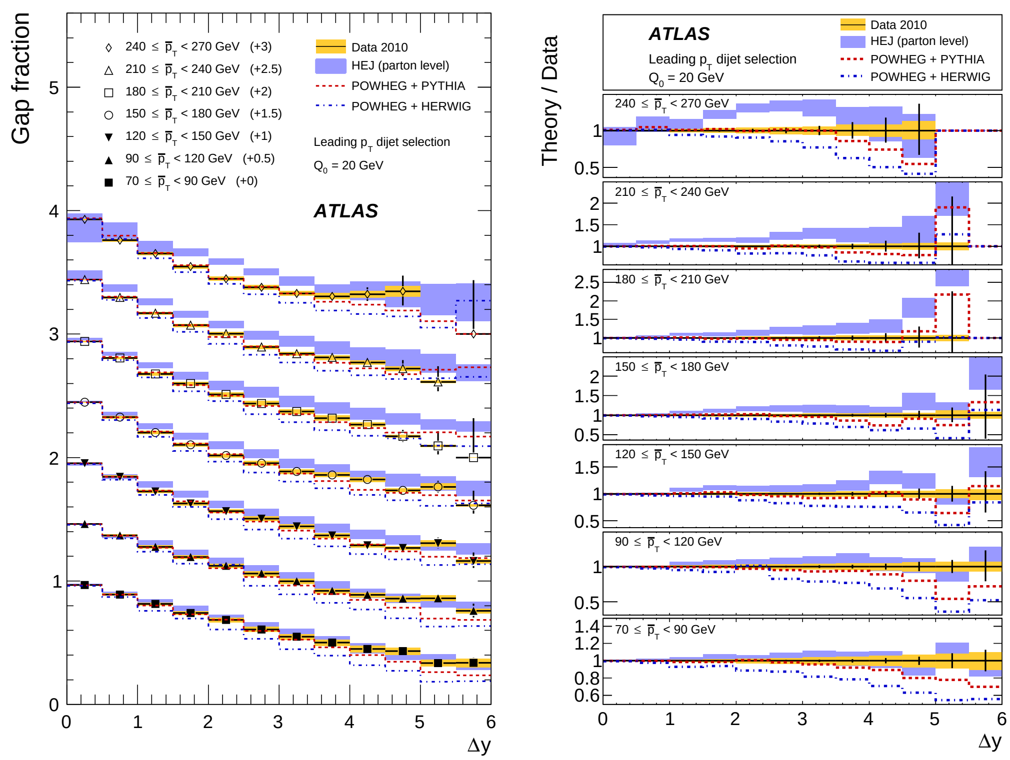

(a) (b)

Figure 6: Gap fraction as a function of Δy for different slices in $\bar{p}_T$ (a) and ratio of theory to data (b). Corrected data with statistical error bars in black and yellow systematic uncertainty band are compared to POWHEG with PYTHIA (red dash) and POWHEG with PHOJET (blue dot). The dark blue band represents theoretical uncertainty in HEJ from variation of the PDF and renormalisation scale.

[4] P. D. B. Collins, *An introduction to Regge theory and high-energy physics / by P. D. B. Collins*. Cambridge University Press, Cambridge [Eng.] ; New York :, 1977.

[5] H1 Collaboration, A. Aktas et al., *Measurement and QCD analysis of the diffractive deep- inelastic scattering cross-section at HERA*, Eur. Phys. J. **C48** (2006) 715–748, `arXiv:hep-ex/0606004`.

[6] S. M. T. Sjostrand and P. Skands, *Brief Introduction to PYTHIA 8.1*, Comput. Phys. Comm. **178** (2008) , `arXiv:0710.3820`.

[7] R. Engel, *Photoproduction within the two component dual parton model. 1. Amplitudes and cross-sections*, Z. Phys. **C66** (1995) 203–214.

[8] A. Kaidalov, V. A. Khoze, A. D. Martin, and M. Ryskin, *Probabilities of rapidity gaps in high-energy interactions*, Eur.Phys.J. **C21** (2001) 521–529, `arXiv:hep-ph/0105145 [hep-ph]`.

[9] *Measurement of the Inelastic Proton-Proton Cross Section at sqrts = 7 TeV with the ATLAS Detector*, Tech. Rep. ATLAS-CONF-2011-002, CERN, Geneva, Feb, 2011.

[10] ATLAS Collaboration, G. Aad et al., *The ATLAS Experiment at the CERN Large Hadron Collider*, JINST **3** (2008) S08003.

[11] *Studies of Diffractive Enhanced Minimum Bias Events in ATLAS*, Tech. Rep. ATLAS-CONF-2010-048, CERN, Geneva, Jul, 2010.

[12] ATLAS Collaboration, G. Aad et al., *Measurement of dijet production with a veto on additional central jet activity in pp collisions at sqrt(s)=7 TeV using the ATLAS detector*, `arXiv:1107.1641 [hep-ex]`.

[13] I. Balitsky and L. Lipatov, *The Pomeranchuk Singularity in Quantum Chromodynamics*, Sov.J.Nucl.Phys. **28** (1978) 822–829.

[14] J. R. Andersen and J. M. Smillie, *High Energy Description of Processes with Multiple Hard Jets*, Nuclear Physics B - Proceedings Supplements **205-206** (2010) no. 0, 205 – 210.

[15] S. Alioli, P. Nason, C. Oleari, and E. Re, *A general framework for implementing NLO calculations in shower Monte Carlo programs: the POWHEG BOX*, JHEP **1006** (2010) 043, `arXiv:1002.2581 [hep-ph]`.

[16] J. Forshaw, J. Keates, and S. Marzani, *Jet vetoing at the LHC*, Journal of High Energy Physics **2009** (2009) no. 07, 023.